

To be published in
Physics Letters

Geneva - 18 April 1977

EXPERIMENTAL COMPARISON OF J/ψ PRODUCTION
BY π[±], K[±], p AND p̄ BEAMS AT 39.5 GeV/c

M.J. Corden, J.D. Dowell, D. Eastwood, J. Garvey, R.J. Homer, M. Jobses, I.R. Kenyon, T. McMahon, R.J. Vallance, P.M. Watkins and J.A. Wilson
Birmingham University, Birmingham, U.K.

J. Gago^(*), M. Jung^(**), P. Sonderegger, D. Treille and P.L. Woodworth
CERN, European Organization for Nuclear Research, Geneva, Switzerland.

V. Eckardt, J. Fent, K. Pretzl, P. Seyboth and J. Seyerlein
Max Planck Institut für Physik und Astrophysik, München, Germany.

D. Perrin
University of Neuchâtel, Neuchâtel, Switzerland.

B. Chaurand, G. de Rosny, L. Fluri, A. Romana, R. Salmeron and
A. Wijangco
Ecole Polytechnique, Palaiseau, France.

K.C.T.O. Sumorok
Rutherford Laboratory, Oxfordshire, U.K.

ABSTRACT

Measurements have been made of relative production cross sections of the J/ψ by π[±], K[±], p and p̄ at 39.5 GeV/c incident on copper. J/ψ production rates from π⁻, K⁻ and p̄ are similar. The J/ψ relative particle/anti-particle production cross sections for x > 0 are σ(π⁺)/σ(π⁻) = (0.87 ± 0.14), σ(K⁺)/σ(K⁻) = (0.85 ± 0.5) and σ(p)/σ(p̄) = (0.15 ± 0.08). The small p/p̄ cross section ratio disagrees with models of J/ψ production by gluon amalgamation.

(*) On leave from the I.S.T., University of Lisbon, Lisbon, Portugal.

(**) On leave from Bonn University, Bonn, Germany.

There has been considerable speculation as to the production mechanism of the $J/\psi(3100)$ in hadronic interactions⁽¹⁻⁴⁾. Large differences should exist between the proton and anti-proton induced cross sections if valence quark annihilation contributes significantly to J/ψ production. Clear differences have been observed between J/ψ production with pion and proton beams both in cross sections and in the distributions of the produced J/ψ in the Feynman x variable⁽⁵⁻⁹⁾.

The aim of the experiment reported here was to measure J/ψ production by π^\pm , K^\pm , p and \bar{p} beam particles in the same large acceptance apparatus. The production of the J/ψ decaying into $\mu^+\mu^-$ was measured at 39.5 GeV/c using both negative and positive unseparated beams from the CERN SPS incident on a copper target located in the Omega spectrometer⁽¹⁰⁾. Production of J/ψ was observed with all six beam particles (π^\pm , K^\pm , p and \bar{p}) and relative cross sections have been obtained for J/ψ production for $x > 0$ using the Feynman x variable $x = 2 p_L^* / \sqrt{s}$ where p_L^* is the centre of mass longitudinal momentum of the muon pair, and \sqrt{s} is the centre of mass energy.

The apparatus, shown schematically in fig. 1, was designed to detect muon pairs with high efficiency for $x > 0$. Three threshold Cerenkov counters were used to identify incident beam particles. Scintillation counters S1-S4 defined the incident beam with V2 and V4 providing protection against beam tails and halo muons. The target consisted of five 4cm thick copper slabs interleaved with scintillation counters T1-T6. Pulse height information was recorded from all Cerenkov, beam and target counters. A 1.46m thick copper absorber immediately after the target reduced the hadron flux by a factor of thirty. Particles emerging from the absorber were detected with a four-element scintillation counter hodoscope, S6, 1.5m wide and 1.0m high. A small counter, V0, was used to veto beam muons. There were three planes of multiwire proportional chambers (Y1, Z2 and Y3 with vertical, horizontal and vertical wires respectively) which were used to provide a particle multiplicity requirement and to reduce $\mu^+\mu^-$ pairs of masses below $1.4 \text{ GeV}/c^2$. Particle trajectories were recorded with a TV readout of forty optical spark chamber gaps, in a region of 1.7T average magnetic induction. Particles leaving the chamber system passed into the 1.25m thick iron return yoke of the magnet which acted as a second hadron absorber before a final counter hodoscope of sixty elements covering an area 6m wide and 3.8m high.

The spark chambers were triggered when the following conditions were satisfied:

- (a) a single incident beam hadron (defined by S1, S2, S3, S4, $\overline{V0}$, $\overline{V2}$, $\overline{V4}$) was present with no other beam particle within ± 20 nsecs;
- (b) the final counter of the target (T6) had a pulse height greater than 1.3 times that of an average single particle;
- (c) a signal was present from S6 (this was used in strobing the multiwire chambers);
- (d) signals were present from two non-adjacent elements in the final hodoscope situated downstream of the magnet return yoke;
- (e) there was a multiplicity of two or three in the multiwire planes Y1 and Z2;
- (f) for incident pions only, and if the multiplicity was two, triggers from low mass muon pairs were effectively reduced by requiring either a vertical separation between hits in multiwire chamber Z2 larger than 30cm, or an appropriate correlation between the horizontal separations ($\Delta Y1, \Delta Y3$) of hits in multiwire planes Y1 and Y3.

In a twenty day run 445,000 triggers were recorded with negative beam and 201,000 with positive beam. The beam intensity was limited to 3×10^6 in an effective spill of 300ms. The trigger rate was 10 per burst. Beam fractions were 93.9% π^- , 3.4% K^- , 2.7% \bar{p} ; and 72.2% π^+ , 3.7% K^+ and 24.1% p. The total amounts of gated negative and positive beam were 4.0×10^{10} and 1.4×10^{10} respectively.

All triggers were processed through a modified version of the offline pattern recognition and geometric reconstruction program ROME0⁽¹¹⁾. The single spark resolution was 500 μ m in space and the efficiency for reconstructing muon tracks exceeded 95%. In order to locate the vertex of the interaction to within a target element, the program used the pulse heights from counters T1 to T6. The resulting distribution of interactions through the target was consistent with the known cross sections in copper. Each track reconstructed in the spark chambers was extrapolated back to the appropriate target element centre plane taking into account the energy losses.

The track was discarded if its displacement from the beam axis was inconsistent with multiple scattering errors. The correlation between mean angular and position displacements arising from multiple scattering was used to reduce the average errors on the angles of the extrapolated tracks. This procedure reduced the error on the muon pair effective mass by a factor of 1.6 and yielded a J/ψ width consistent with the Monte Carlo estimate of $0.35 \text{ GeV}/c^2$.

The negative and positive beam data yielded 2009 and 418 events respectively containing a $\mu^+\mu^-$ pair with effective mass above $1.6 \text{ GeV}/c^2$ and satisfying the following criteria:

- (a) both tracks come from a common vertex as described earlier and have associated hits in the final hodoscope;
- (b) the momentum of each muon was less than $30 \text{ GeV}/c$ and the sum of the two momenta did not exceed the beam momentum within measurement errors;
- (c) the reconstructed track length in the spark chambers was greater than 20cm for each track.

The $\mu^+\mu^-$ mass spectra produced by π^- and π^+ beams shown in fig. 2 exhibit clear J/ψ signals with masses 3.12 and $3.15 \text{ GeV}/c^2$ and FWHM's $0.43 \text{ GeV}/c^2$ and $0.36 \text{ GeV}/c^2$ respectively. We can put an upper limit on ψ' production and decay to $\mu^+\mu^-$ of 4% of the J/ψ rate and we ignore it hereafter. With the above criteria there are 8 and 2 like sign muon pairs in the mass range $2.7 - 3.5 \text{ GeV}/c^2$ for negative and positive beam, roughly 1% of the respective J/ψ signals. In figs. 3(a) and (b) we display the dN/dx distribution of $\mu^+\mu^-$ events in the J/ψ region ($2.7 < M_{\mu\mu} < 3.5 \text{ GeV}/c^2$) for π^- and π^+ beams respectively. The data points are corrected for acceptance assuming that J/ψ production is unpolarized. Fig. 4 shows the distributions of dN/dp_T^2 for $x > 0$ and the same mass range. These are well fitted by the form $Ae^{-Bp_T^2}$ where $B = (1.3 \pm 0.1)$ and $(1.5 \pm 0.2) (\text{GeV}/c)^{-2}$ for π^- and π^+ induced J/ψ 's respectively. In a previous experiment with a π^- beam at $43 \text{ GeV}/c$ ⁽⁸⁾, a similar slope B of $(1.7 \pm 0.4) (\text{GeV}/c)^{-2}$ was found, while substantially lower values have been obtained with pion beams at higher energies⁽¹²⁾.

The mass distributions for $\mu^+\mu^-$ pairs produced by K^- , K^+ , \bar{p} and p are also shown in Fig. 2. All exhibit clear enhancements at the J/ψ mass. Strong signals from $\rho/\omega \rightarrow \mu\mu$ and, for K^\pm beams only, shoulders from $\phi \rightarrow \mu\mu$ signals can also be seen. Every event appearing in fig. 2 with muon pair mass above $2.4 \text{ GeV}/c^2$ has been examined carefully for any inconsistencies in the data such as disagreement between Cerenkov pulse height information and discriminator responses.

Table 1(a) shows the number of events with $x > 0$ (and for the restricted range $0 < x < 0.4$) unweighted and weighted for acceptance in the range $2.7 < M_{\mu\mu} < 3.5 \text{ GeV}/c^2$ produced by each minority beam particle. The numbers for π^\pm for $x > 0$ were extracted from Gaussian plus background fits to their unweighted and weighted mass spectra. We have estimated the number of J/ψ produced by each minority beam particle for $x > 0$ in two ways. The first method assumes that all events with $2.7 < M_{\mu\mu} < 3.5 \text{ GeV}/c^2$ are J/ψ and gives an upper limit; the second method assumes a linear background under the J/ψ using the sidebands $2.3 < M_{\mu\mu} < 2.7 \text{ GeV}/c^2$ and $3.5 < M_{\mu\mu} < 3.9 \text{ GeV}/c^2$ and yields a lower limit. The signals obtained from the weighted data by each method for $x > 0$ are shown in table 1(b). The errors quoted are statistical only. In order to convert these numbers to relative cross sections we have used the integrated beam fluxes and compositions quoted above and a $\pm 10\%$ relative normalisation error. Table 1(c) shows the cross sections for J/ψ production relative to that for π^- beam after allowing for a small difference in absorption length in copper for each incident particle. Finally, table 1(d) shows the same result expressed as particle/anti-particle ratios. If the mass dependence of the background above $2.3 \text{ GeV}/c^2$ were widely different between particles and antiparticles the quoted errors would increase.

We obtain an estimate for the absolute cross section for π^- induced J/ψ production with $x > 0$ of $910 \pm 190 \text{ nb/copper nucleus}$. Assuming a linear A dependence this corresponds to $14 \pm 3 \text{ nb/nucleon}$. This is consistent with the value obtained by Antipov et al⁽⁸⁾.

To summarise, we have found that for J/ψ production on copper at 39.5 GeV/c beam momentum for $x > 0$:

$$\sigma(\pi^-) : \sigma(K^-) : \sigma(\bar{p}) = 1 : 1.0 \pm 0.3 : 1.0 \pm 0.3$$

Rough equality between these cross sections is expected in quark annihilation models^(1,2). The particle/antiparticle ratios are again for $x > 0$:

$$\begin{aligned}\sigma(\pi^+) / \sigma(\pi^-) &= 0.87 \pm 0.14, \\ \sigma(K^+) / \sigma(K^-) &= 0.85 \pm 0.50 \quad \text{and} \\ \sigma(p) / \sigma(\bar{p}) &= 0.15 \pm 0.08.\end{aligned}$$

This first measurement of the p/\bar{p} ratio is particularly interesting as it is predicted to be widely different in different models. In the quark annihilation model of Donnachie and Landshoff⁽¹⁾ the \bar{p} induced production of J/ψ is enhanced over the p induced production at our relatively low beam momentum by the large valence quark contribution. Our ratios are consistent with their predictions. Fritzsche⁽³⁾ in a similar calculation which neglects the contribution of charmed quarks in the sea obtains a very small p/\bar{p} ratio for small x . Ellis, Einhorn and Quigg⁽⁴⁾ have discussed the J/ψ production ratios for hadrons and their anti-particles arising from gluon amalgamation and predict each ratio to be unity. This is in clear disagreement with our p/\bar{p} ratio.

We thank the SPS crew for their extra efforts at the beginning of the machine operation, the EA and EP mechanics groups, and the staff of the Omega Spectrometer. We thank also Dornach Metallwerk AG of Dornach, Switzerland, for lending us the copper for the absorber.

References

1. A. Donnachie and P.V. Landshoff, Nuclear Physics B112 (1976) 233, also private communication.
2. D. Sivers, Nuclear Physics, B106 (1976) 95, also private communication.
3. H. Fritzsch, Calt 68-582, January 1977.
4. S.D. Ellis, M.B. Einhorn and C. Quigg, Physical Review Letters 36 (1976) 1263.
5. K.J. Anderson et al., Physical Review Letters 36 (1976) 237.
6. K.J. Anderson et al., "Production of the J(3.1) and $\psi'(3.7)$ by 225 GeV π^+ , π^- and protons", submitted to the Tbilisi Conference 1976.
7. G.J. Blamar et al., Physical Review Letters 35 (1975) 346.
8. Yu. M. Antipov et al., "Dimuon Production by 43 GeV/c negative Particles", Tbilisi-Moscow Preprint.
9. Yu. M. Antipov et al., Physics Letters 60B (1976) 309.
10. O. Gildemeister, International Conference on Instrumentation for High Energy Physics, Frascati 1973.
11. F. Bourgeois, H. Grote and J-C. Lassalle. Pattern Recognition Methods for Omega and SFM Spark Chamber Experiments, CERN/DD/DH/70-1. H. Grote, M. Hansroul, J-C. Lassalle and P. Zanella, Identification of Digitized Particle Trajectories, International Computing Symposium, 1973 (North-Holland, 1974).
12. D. Hitlin, SLAC - PUB - 1869 (1977).

Figure Captions

Figure 1: Schematic layout of the apparatus.

Figure 2: Observed $\mu^+\mu^-$ effective mass spectra from π^\pm , K^\pm , p and \bar{p} beams. The π^\pm data are depressed at low masses by the trigger and are shown above $1.6 \text{ GeV}/c^2$ only. Arrows denote the masses of the ρ , ϕ and ψ mesons. For ease of display, different scales are used for nucleon and meson induced events.

Figure 3: dN/dx distributions for $\mu^+\mu^-$ pairs of effective mass $2.7 < M_{\mu\mu} < 3.5 \text{ GeV}/c^2$ (a) for π^- beam (b) for π^+ beam. The histograms show the raw data. The points, with statistical errors only, represent the data corrected for acceptance.

Figure 4: dN/dp_T^2 distributions of $\mu^+\mu^-$ pairs of effective mass $2.7 < M_{\mu\mu} < 3.5 \text{ GeV}/c^2$ and $x > 0$ for π^- and π^+ incident beam after correction for acceptance. The fits are of the form $Ae^{-Bp_T^2}$ in the range $0 < p_T^2 < 2.0 \text{ (GeV}/c)^2$.

Table 1 (as explained in the text)

	π^-	π^+	K^-	K^+	\bar{p}	p
(a) Number of events in J/ψ region for $x > 0$	700 ± 42	179 ± 16	30	7	22	10
Number of events in J/ψ region for $x > 0$ weighted for acceptance	1850 ± 140	434 ± 44	73	24	65	29
Number of events in J/ψ region for $0.4 > x > 0$	471 ± 30	108 ± 14	19	6	19	7
Number of events in J/ψ region for $0.4 > x > 0$ weighted for acceptance	1322 ± 106	297 ± 33	50	22	58	24
(b) J/ψ signal $x > 0$			73 ± 13	24 ± 9	65 ± 14	29 ± 9
Method 1						
Method 2			58 ± 16	17 ± 11	53 ± 16	27 ± 10
(c) J/ψ cross section relative to that for π^- beam for $x > 0$	1	0.87 ± 0.14	1.1 ± 0.2	1.0 ± 0.4	1.1 ± 0.2	0.16 ± 0.05
Method 1						
Method 2			0.9 ± 0.2	0.7 ± 0.5	0.9 ± 0.3	0.14 ± 0.05
(d) Particle/Antiparticle ratio for J/ψ for $x > 0$			0.9 ± 0.4		0.15 ± 0.06	
Method 1						
Method 2	0.87 ± 0.14		0.8 ± 0.5		0.16 ± 0.08	



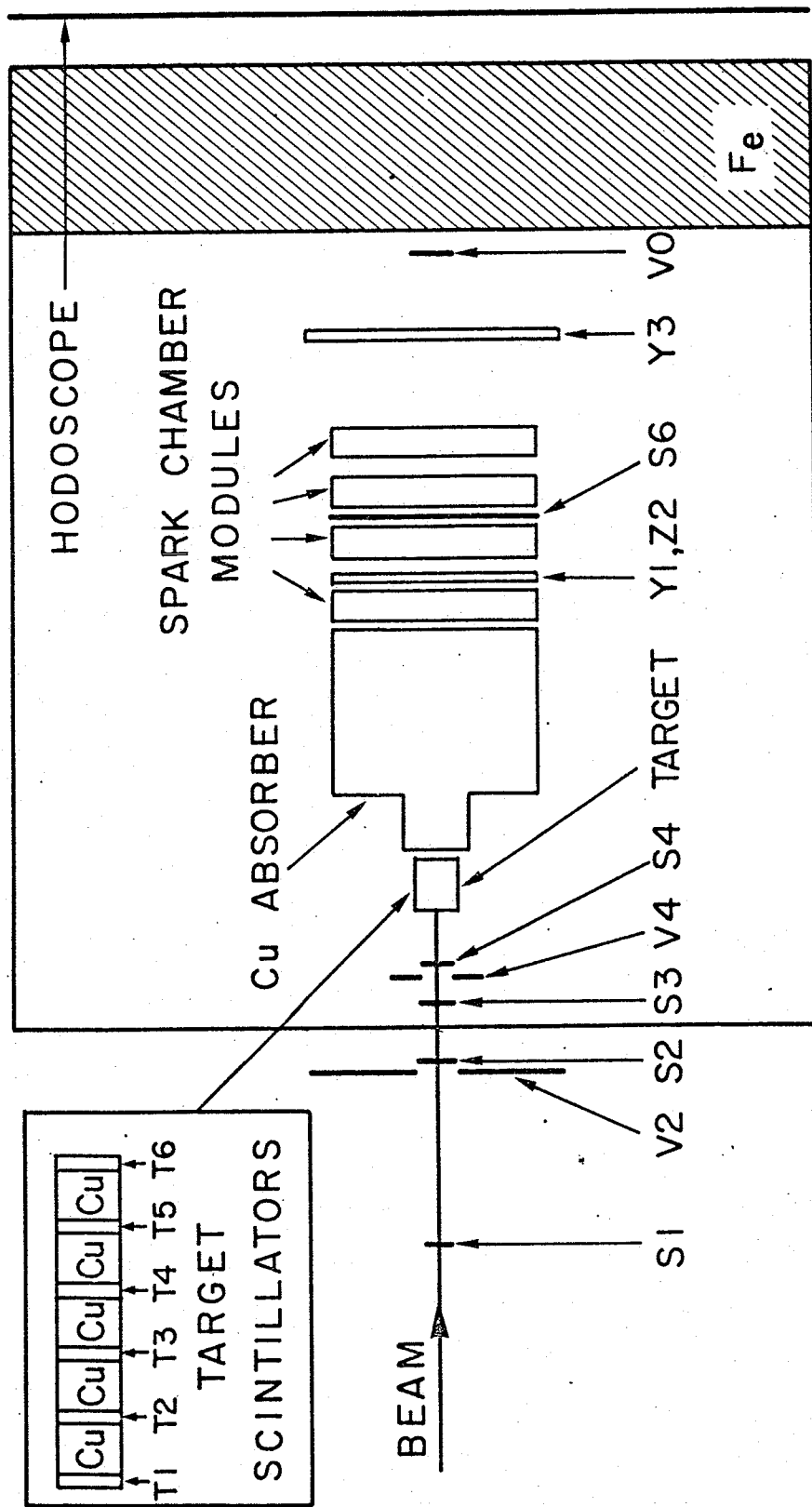
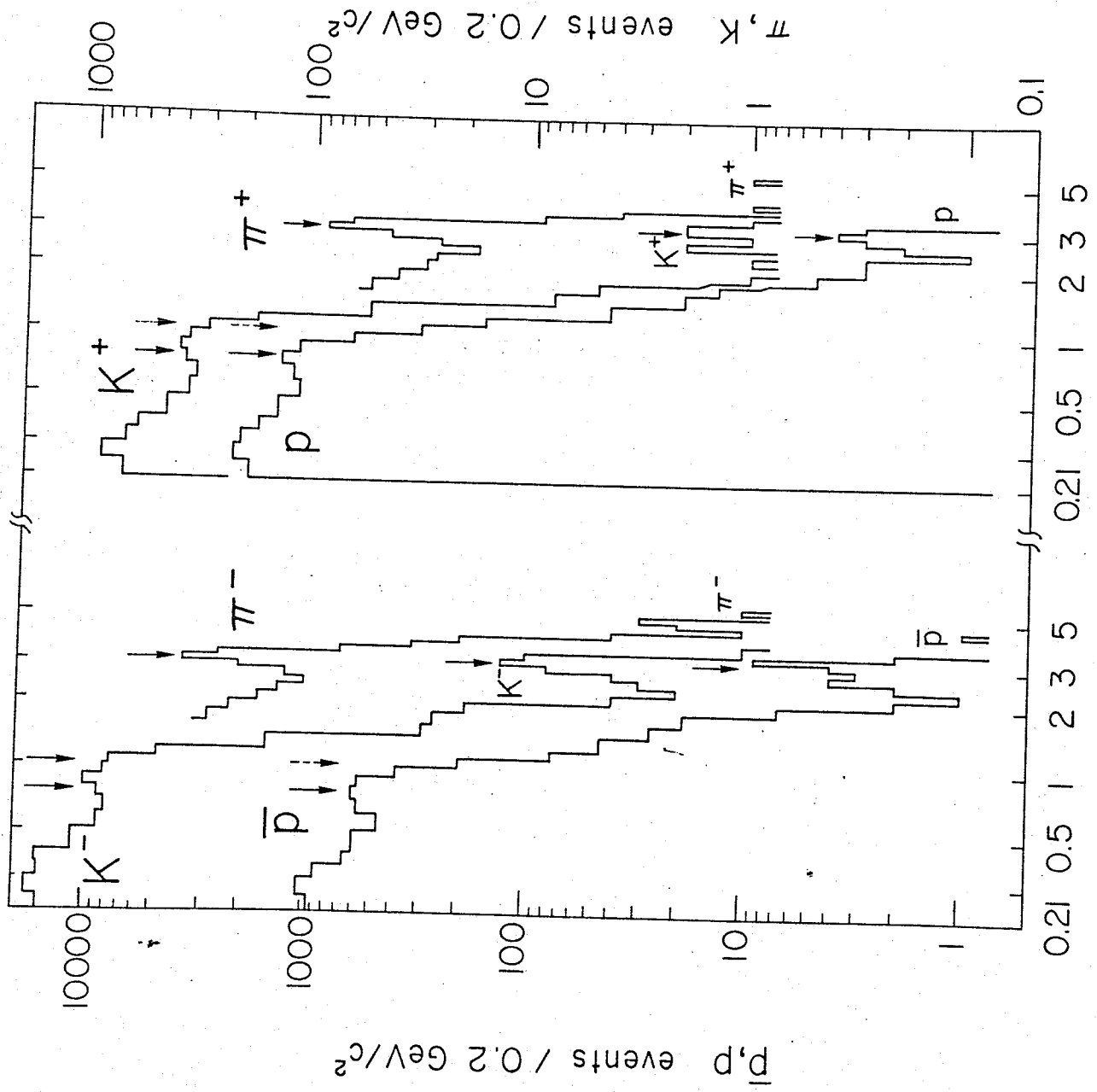


Fig. 1



$M_{\mu^+\mu^-}$ [GeV/c^2]

Fig: 2

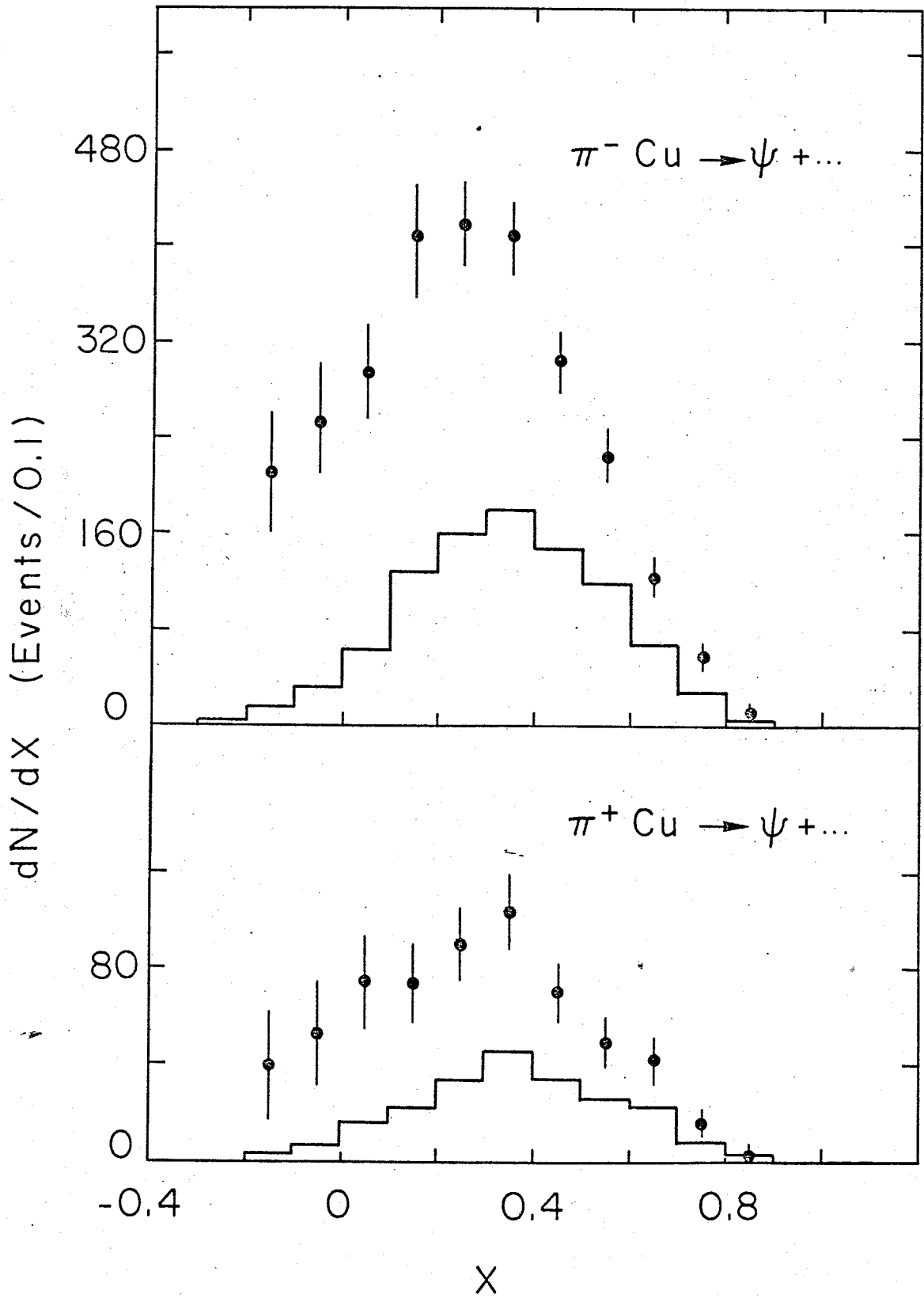


Fig. 3

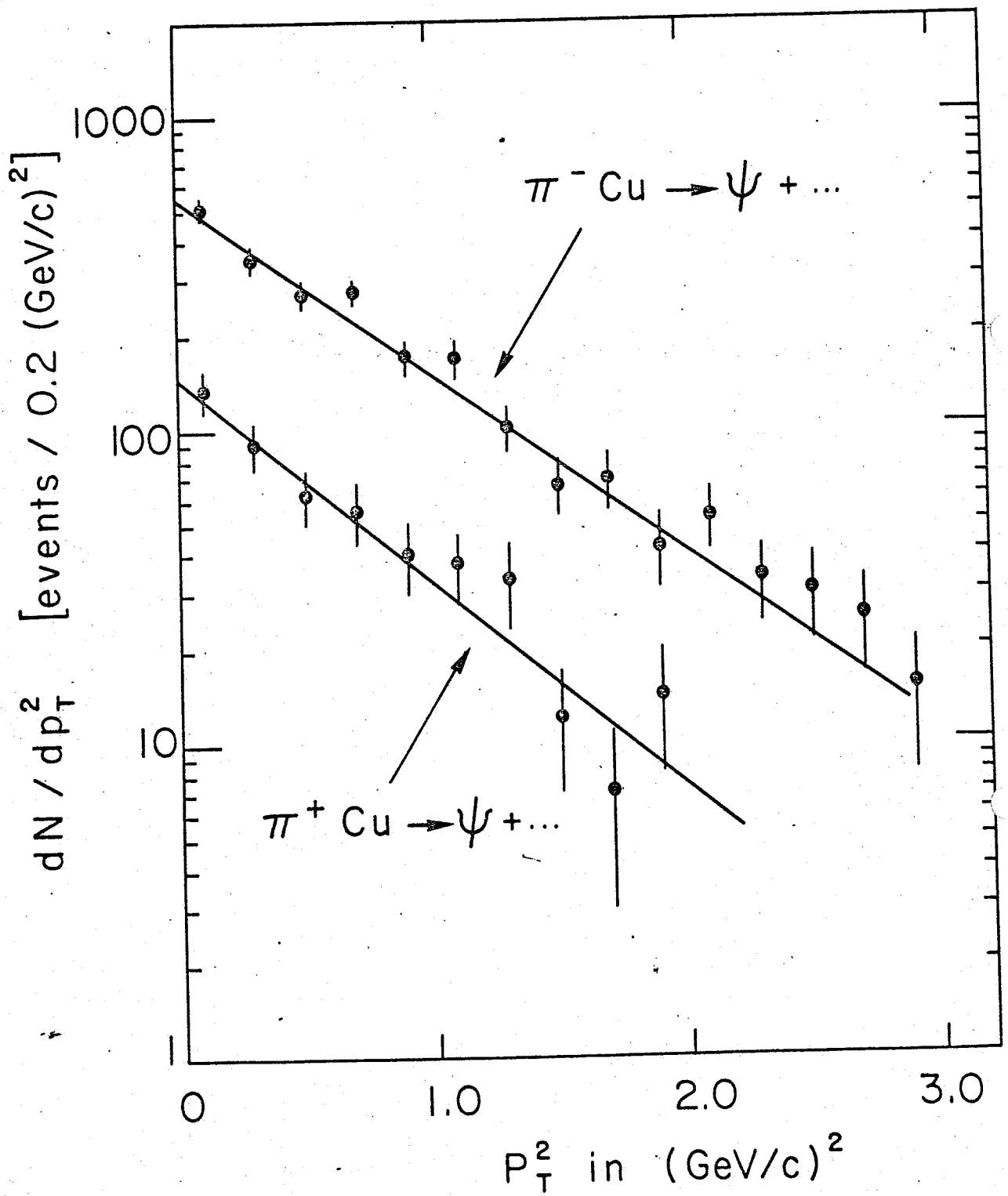


Fig. 4